Real-Time Fluorescence Lifetime Actuation for Cell Sorting using a CMOS SPAD Silicon Photomultiplier

FRANCESCOPAOLO MATTIOLI DELLA ROCCA[1,4,*], JAKUB NEDBAL[2], DAVID TYNDALL[3], NIKOLA KRSTAJIĆ[1], DAVID DAY-UEI LI[5], SIMON M. AMEER-BEG[2], AND ROBERT K. HENDERSON[1]

[1] CMOS Sensors and Systems, Institute for Integrated Micro and Nano Systems, School of Engineering, University of Edinburgh, Edinburgh, UK
[2] Division of Cancer Studies & Randall Division of Cell and Molecular Biophysics, Guy's Campus, King's College London, London, UK
[3] Dialog Semiconductor, 2 Multrees Walk, Edinburgh, UK
[4] STMicroelectronics Imaging Division, 33 Pinkhill, Edinburgh, UK
[5] Centre for Biophotonics, Strathclyde Institute of Pharmacy & Biomedical Sciences, University of Strathclyde, 161 Cathedral Street, Glasgow, UK
[*] Corresponding author: francesco.mattiolidellarocca@ed.ac.uk

Compiled December 26, 2015

Time-correlated single photon counting (TCSPC) is a fundamental fluorescence lifetime measurement technique offering high signal to noise ratio (SNR). However, its requirement for complex software algorithms for histogram processing restricts throughput in flow cytometers and prevents on-the-fly sorting of cells. We present a single-point digital Silicon Photomultiplier (SiPM) detector accomplishing real-time fluorescence lifetime-activated actuation targeting cell sorting applications in flow cytometry. The sensor also achieves burst-integrated fluorescence lifetime (BIFL) detection by TCSPC. The SiPM is a single-chip complementary metal oxide semiconductor (CMOS) sensor employing a 32×32 single-photon avalanche diode (SPAD) array and 8 pairs of time-interleaved time to digital converters (TI-TDCs) with a 50 ps minimum timing resolution. The sensor's pile-up resistant embedded centre of mass method (CMM) processor accomplishes low-latency measurement and thresholding of fluorescence lifetime. A digital control signal is generated with a 16.6 µs latency for cell sorter actuation allowing a maximum cell throughput of 60,000 cells per second and an error rate of 0.6%.

OCIS codes: *(040.5160) Photodetectors; (030.5260) Photon counting; (170.3650) Lifetime-based sensing; (170.6280) Spectroscopy, fluorescence and luminescence; (040.3780) Low light level.*

Measurement of fluorescence lifetime is a well-established experimental technique to probe protein-protein interactions occurring in live cells [1]. In flow cytometry it can be used as a parameter to isolate sub-populations of cells from a heterogeneous sample by a method called Fluorescence Activated Cell Sorting (FACS) [2]. To provide the ability to measure the fluorescence lifetime of fluorophores to nanosecond precision, various time-resolved methods have been proposed [3]. Amongst these techniques Time-Correlated Single Photon Counting (TCSPC) provides a method to time single photon arrivals with high resolution and efficiency [4].

The limiting factor of sorting techniques in flow cytometry is the complexity and the large volume of fluorescence data to be processed to detect the passage of each individual cell and identify its chemical or physical characteristics to perform a reliable sorting decision. For this reason, existing time-resolved fluorescence lifetime flow cytometers such as reported in [5] and [6] do not perform cell sorting. Processing of the fluorescence signal is performed offline on a PC causing large delays from slow data transfer rates. In addition, phase-filtered sorting cytometers such as presented in [7] report low lifetime resolution preventing cell populations with similar lifetimes to be distinguished.

Recent advances in Complementary Metal Oxide Semiconductor (CMOS) sensors have permitted the integration of complete Silicon Photomultiplier (SiPM) detectors with high-resolution timing directly on-chip [8] as well as fast communication with embedded systems such as field programmable gate arrays (FPGAs) offering greatly reduced transfer rates and eliminating the requirement of a PC for data processing. We present a SPAD-based SiPM detector, which to the best of our knowledge is the first sensor able to perform low-latency time-resolved fluorescence lifetime measurement and online sorting decisions to drive an actuation system for fluorescence lifetime cytometric sorting. The SiPM is implemented on a single-chip 1.3 mm by 1.7 mm in size and includes a 32×32 SPAD array with 10% fill factor [8]. The sensor encompasses two modalities: (1) a time continuous burst-integrated fluorescence lifetime (BIFL) TCSPC histogramming system targeting cytometric studies and sorting calibration and (2) a real-time sorting actuation system based on FPGA embedded Centre of Mass Method (CMM) lifetime computation and thresholding.

In TCSPC photon arrival times are converted into a representation of the captured fluorescence intensity decay curve. Short laser pulses give rise to fluorescence emission in the sample. The time delay between the fluorescence detection with respect to the excitation pulse that triggered the fluorescence is measured and converted into a digital signal which is then used to build a

histogram of photon counts as a function of photon arrival time. Each histogram is fitted with an exponential model to estimate the fluorescence lifetime of the sample [3].

The TCSPC system on the SiPM is composed of a pair of time-interleaved time to digital converters (TI-TDCs) performing high-resolution timing. TI-TDCs output the photon arrival times in the form of 10-bit time stamps during an exposure to a parallel bus, which directly links to the FPGA. Histograms representing the fluorescence decay are accumulated for a user-preset exposure time by incrementing counters in the FPGA memory addressed by the photon time stamps. During the experiment, the contents of the memory are continuously transferred to a PC to calculate the fluorescence intensity and fluorescence lifetime for each exposure. A diagram of the TCSPC system on the SiPM is shown in Fig. 1.

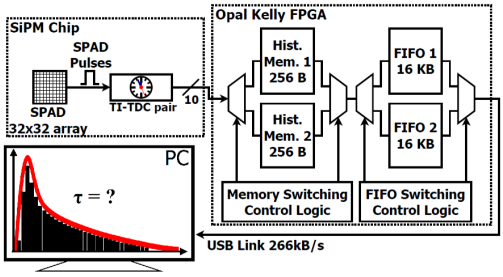

Fig. 1. Time-continuous BIFL TCSPC system diagram showing the fluorescence detection and timing system on-chip, the alternating memories for histogramming on FPGA and FIFO buffers to transfer the histograms via USB for exponential fitting and lifetime calculation on PC.

On the FPGA, two time-interleaved 256 byte histogramming memories are composed of 256 addresses with an 8-bit counter per address allowing collection of photons in 256 time-bins for each exposure. The time resolution of the histogram bins in the memory is set by the TDC resolution and is user-configurable to be between 50 ps and 3.2 ns giving a timing dynamic range of each histogram from a minimum 12.8 ns up to 0.82 µs. Two time-multiplexed histogramming memories and first-in, first-out (FIFO) buffers are implemented to enable continuous histogram accumulation in one memory while the content of the other is being transferred to the PC. The FIFO memories are 16 KB each allowing storage of up to 512 histograms per FIFO before transfer to PC. The read-out rate of the USB is 266 kB/s enabling continuous detection with no time-gaps in photon capture between successive exposures with a minimum 1 ms exposure time. The histogram is processed in software by an adapted version of the DecayFit exponential fitting algorithm [9, 10] in MATLAB to compute the fluorescence lifetime recorded for each exposure.

The Centre of Mass Method (CMM) is an averaging algorithm for fluorescence lifetime approximation [11]. It is embedded in the SiPM hardware, allowing low-latency fluorescence lifetime estimation, thresholding and direct sorting control without the requirement for transfer to a host PC [8, 11]. The method calculates fluorescence lifetime by averaging the photon arrival times measured by the on-chip TDCs. The arrival times N_i within each time-bin i are summed and divided by the total number of photon events N_c detected in an exposure to obtain a first-order approximation of the lifetime τ as shown in Eq. 1 [11].

$$\tau = \frac{\sum_{i=0}^{M} i \cdot N_i}{N_c} \quad \textbf{(1)}$$

The low-latency lifetime computation and thresholding system is partitioned between hardware on-chip for photon event accumulation and firmware for CMM division and generation of the sorting actuation on FPGA as shown by the system diagram in Fig. 2.

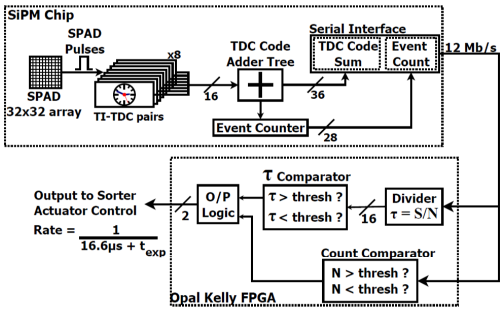

Fig. 2. Diagram of the embedded CMM processor and actuation system partitioned between chip and FPGA. Photon detection, timing and precalculation of TDC code sum and photon event count occur on-chip. FPGA performs CMM division, thresholding and generation of the sorting actuation signal.

A ripple counter counts the number of photon events that fall within a user-set time window storing the result in a 28-bit accumulator. The time stamps of the detected photon events output from the 8 pairs of CMM-dedicated TI-TDCs are summed by an adder tree and stored into a 36-bit accumulator [8].

The pre-calculated arrival time sum and total photon count collected in an exposure are concatenated into a 64-bit number, which is streamed at 12 Mb/s from an on-chip serial interface (SI) directly to the FPGA with a transfer delay of only 5.3 µs per exposure. The total number of photons detected in each exposure is monitored on the FPGA and a thresholding function interrupts data transfer and processing for exposures with photon counts recorded below the background noise level. This allows the system to signal the absence of a specimen through the cytometer focal volume.

To obtain the fluorescence lifetime from the CMM data received from the chip, a divider is implemented on FPGA which performs the division in Eq. 1. The division operation is based on a long-division firmware algorithm as proposed in [12], which performs iterative subtractions of the total photon count from the time-code sum checking the sign of the difference at each subtraction. Each subtraction iteration is completed within 2 FPGA clock cycles amounting to a total worst-case division and thresholding delay of 11.3 µs when operating at 48 MHz FPGA system clock rate. This time combined with the 5.3 µs SI delay means that the lifetime result can be available to the sorter after only 16.6 µs from the end of the exposure. Since the lifetime calculation is done on FPGA there is only a 5.3 µs delay between the end of one exposure and the next allowing the SiPM to start a new exposure without being affected by processing delays.

The FPGA generates an actuation signal for downstream cell sorting hardware by comparing the fluorescence lifetime result obtained at the end of the iterative subtractions against a user-set programmable lifetime threshold. If the lifetime result is below the sorting threshold a binary 1 is output at the pins of the FPGA, while if the lifetime is found to be above threshold a binary 2 is output. Binary 3 is output when no lifetime is recorded due to the photon counts being below the noise-level count threshold.

The SiPM was tested and characterised in laser-scanning ex-

periments using samples of two different fluorophore-tagged microparticles. Melamine FITC-stained microparticles in a 1.91×10^7 particle/ml suspension (Sigma-Aldrich, Irvine, UK) are 10 µm in diameter and feature a fluorescence lifetime of 4.1 ± 0.1 ns [13]. Latex Firefli-stained microparticles in a 2.78×10^9 particles/ml suspension (Thermo Scientific, Waltham, MA) are 1.9 µm in diameter with a fluorescence lifetime of 2.0 ± 0.2 ns [5]. 0.1 mm-internal diameter capillaries (VitroCom, Mountain Lakes, NJ) containing undiluted suspensions of the fluorescent microparticles were positioned close and parallel to each other on a microscope slide as shown in Fig. 3. Capillaries were sealed at both ends with epoxy resin to prevent solvent evaporation.

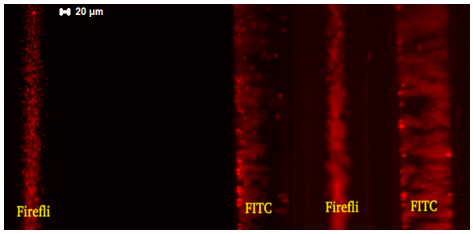

Fig. 3. Microscope image of capillaries containing fluorescent microparticles stained with Firefli and FITC fluorophores arranged on a slide in alternating pattern. The variable granularity is due to the varying axial positioning of each capillary leading to blurring of out-of-focus microparticles. 20 µm scale bar. Capillary internal diameter equal to 0.1 mm, outer diameter equal to 0.17 mm.

A diagram of the experimental setup is shown in Fig. 4. The excitation source is a 473 nm, 20 MHz pulsed laser BDL-473-SMC (Becker & Hickl GmbH, Berlin, Germany) with an average power of 0.2 mW. A scanning microscope stage is controlled through the SPC-830 TCSPC Imaging Module (Becker & Hickl GmbH, Berlin, Germany). The laser beam was scanned across the microscope slide and the detector captured the fluorescence light for 1000 exposures of 10 ms each. The photon bursts detected were processed and the fluorescence lifetime for each exposure was plotted as a function of time as shown in Fig. 5. The histogram showing the distribution of fluorescence lifetimes detected is shown in Fig. 6.

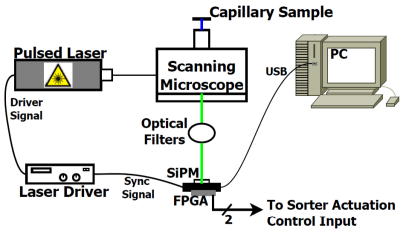

Fig. 4. Diagram of laser-scanning experimental setup for validation of BIFL and lifetime actuation using the SiPM detector. Microscope scanned laser beam across capillary sample and fluorescence was detected by SiPM communicating with FPGA and PC for data transfer.

The plot in Fig. 5 shows the correct identification of each different microparticle population within the capillaries as the microscope scanned across the slide. Analysis of the histogram in Fig. 6 shows two Gaussian distributions representing the detection of the two fluorophore-tagged populations of microparticles. The mean of the populations differ from the quoted lifetimes of the fluorophore by a worst-case 0.2 ns. It was found that the error on the mean and the standard deviation could be further reduced by increasing the detected photon count rate and minimising the noise floor by disabling the SPADs with high dark

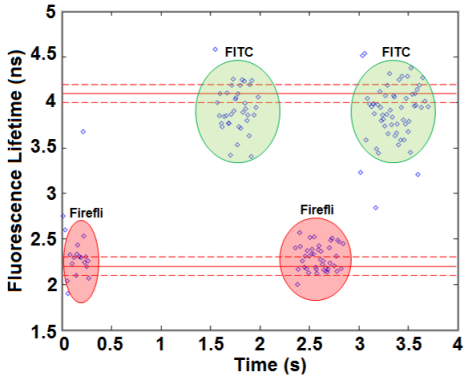

Fig. 5. Measured fluorescence lifetime of photon bursts recorded for the capillary slide scanning in BIFL detection by TCSPC. Two alternating populations identified corresponding to the fluorophores in the capillaries. Average count rate measured equal to 300 kHz. Average dark count rate equal to 800 Hz.

count rate (DCR) while focusing the fluorescence from the illuminated microparticles on the enabled SPADs. To this effect, a reduction of the average DCR per SPAD from 10 kHz to 100 Hz by enabling lower-DCR SPADs, reported an increase in the SNR from 3 to 300. With higher count rates, lower exposures to improve BIFL time resolution can also be accomplished by a more efficient use of the USB peripheral data-rate which can improve the TCSPC maximum exposure rate increasing it above 100 kHz.

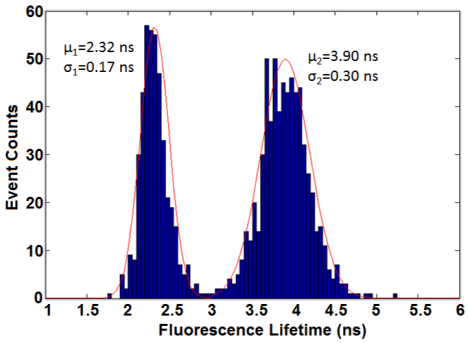

Fig. 6. Histogram of fluorescence lifetime of scanned capillaries. TCSPC exposures identifying the presence of two microparticle populations with lifetimes in the correct ranges for FITC and Firefli.

The same experiment was repeated using the CMM mode of the chip to test the sorting actuation function of the sensor. Actuation bits from the FPGA output pins were recorded and mapped as a function of time for 4000 exposures of 10 ms each as shown in Fig. 7. The experiment was repeated for different exposures and the data analysed to calculate the error rate of the SiPM in outputting the correct actuation bits for the corresponding microparticle type. The error rates measured for the tested exposure times are shown in Table 1. Error rates were calculated by direct comparison of the actuation signal with reference lifetime values obtained from TCSPC histogram measurements of the same sample.

The plot in Fig. 7 shows the ability of the CMM actuation to correctly identify the two populations of microparticles on the slide. The alternating pattern of flurophore-tagged microparticles visible in the intensity signal plot in Fig. 7(a) was replicated in the actuation bit pattern in (b). In this experiment the lifetime actuation threshold was set at 3 ns, midway between the values of the lifetimes quoted for the two fluorophore types allowing

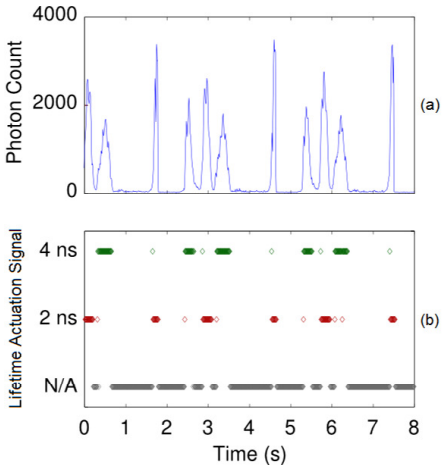

Fig. 7. (a) Intensity signal for each exposure showing successive bursts from fluorescent microparticles in capillaries. (b) Actuation signal for each exposure following the pattern of fluorophores in the capillaries using a 3 ns fluorescence lifetime threshold.

Table 1. Sorting actuation error rates for different exposures.

Exposure Time (ms)	Error Rate (% Exposures)
2	24
10	0.6
20	0.04

the SiPM to differentiate detections between lifetimes below threshold for Firefli-tagged microparticles and above threshold for FITC microparticles. A preliminary TCSPC experiment allowed the measurement of the noise level to set the count threshold below which the CMM actuation signalled the absence of specimen detection (N/A in the plot in Fig. 7).

While the microparticle scanning experiment demonstrated real-time calculation of fluorescence lifetime, thresholding and sorting using the SiPM, the experimental setup cannot completely reproduce a flow cytometry environment with live cells. Due to the clustering of the microparticles in the capillaries, transient peaks of fluorescence originating from multiple microparticles within single exposures yielded a higher count rate than that obtainable from individual cell transitions in flow, thus prompting for solutions to increase the detected SNR.

The maximum sorting rate limit of 60,000 cells per second is set by the CMM actuation delay of 16.6 µs. This figure does not however account for the exposure time necessary to collect enough photons to perform a sorting decision, which is determined by the entire cytometric system including the optics and fluidics as well as the electronics. The minimum exposure time of 2 ms used in the experiment limits the sorting rate to only 500 particles per second. The exposure was set to a high value to obtain a SNR high enough to yield a low error rate in the CMM calculation of lifetime. However, as the noise-level is fixed and is primarily set by the DCR of the SPADs, the detected photon count rate can be increased by selecting lower-DCR SPADs [14] and an optimised optical system employing a microscope to focus the fluorescence signal only over the enabled SPAD area of the SiPM. In addition, the use of a higher frequency pulsed laser also increases the photon count rate allowing the use of smaller exposures in the order of microseconds to better exploit the low-latency CMM embedded lifetime actuation reaching sorting rates greater than tens of thousands of cells per second.

We presented a CMOS 32×32 SPAD array SiPM accomplishing low-latency fluorescence lifetime actuation by CMM and burst detection by TCSPC. Employing 8 pairs of TI-TDCs and splitting the lifetime calculation between a precalculation on-chip and division and thresholding on FPGA, the SiPM is capable of measuring fluorescence lifetime within 16.6 µs with error-rates below 0.6%. The detector's fast embedded calculation of fluorescence lifetime makes it ideal to target novel sorting applications in flow cytometry by an increased throughput, high time resolution and on-the-fly sorting actuation.

Funding. Engineering and Physical Sciences Research Council (EPSRC) (EP/K03197X/1).

Acknowledgements. Work supported by Cancer Research UK, Engineering and Physical Sciences Research Council (UK), Medical Research Council (UK) and Department of Health (UK), KCL/UCL Comprehensive Cancer Imaging Centre (JN), and by The Dimbleby Cancer Care endowment fund to King's College London (SAB). STMicroelectronics for chip manufacturing.

REFERENCES

1. M. Tramier, I. Gautier, T. Piolot, S. Ravalet, K. Kemnitz, J. Coppey, C. Durieux, V. Mignotte, and M. Coppey-Moisan, "Picosecond-hetero-FRET microscopy to probe protein-protein interactions in live cells." Biophysical journal **83**, 3570–7 (2002).
2. R. Cao, V. Pankayatselvan, and J. P. Houston, "Cytometric sorting based on the fluorescence lifetime of spectrally overlapping signals." Opt Express **21**, 14816–14831 (2013).
3. W. Becker, *Advanced Time-Correlated Single Photon Counting Techniques*, vol. 81 (2005).
4. W. Becker, A. Bergmann, M. Hink, K. König, K. Benndorf, and C. Biskup, "Fluorescence Lifetime Imaging by Time-Correlated Single-Photon Counting," Microscopy Research and Technique **63**, 58–66 (2004).
5. J. Nedbal, V. Visitkul, E. Ortiz-Zapater, G. Weitsman, P. Chana, D. R. Matthews, T. Ng, and S. M. Ameer-Beg, "Time-domain microfluidic fluorescence lifetime flow cytometry for high-throughput Förster resonance energy transfer screening," Cytometry Part A **87**, 104–118 (2015).
6. W. Li, G. Vacca, M. Naivar, and J. P. Houston, "Fluorescence Lifetime-Dependent Flow Cytometry in the Time-Domain," in "CYTO," (2013), p. 97.
7. J. P. Houston, M. A. Naivar, and J. P. Freyer, "Digital analysis and sorting of fluorescence lifetime by flow cytometry." Cytometry. Part A. **77**, 861–72 (2010).
8. D. Tyndall, B. R. Rae, D. D.-U. Li, J. Arlt, A. Johnston, J. A. Richardson, and R. K. Henderson, "A High-Throughput Time-Resolved Mini-Silicon Photomultiplier With Embedded Fluorescence Lifetime Estimation in 0.13um CMOS," IEEE Transactions on Biomedical Circuits and Systems **6**, 562–570 (2012).
9. S. Preus, K. Kilså, F. A. Miannay, B. Albinsson, and L. M. Wilhelmsson, "FRETmatrix: A general methodology for the simulation and analysis of FRET in nucleic acids," Nucleic Acids Research **41**, 1–12 (2013).
10. S. Preus, *DecayFit - Fluorescence Decay Analysis Software 1.3*, FluorTools (2014).
11. D.-U. Li, B. Rae, R. Andrews, J. Arlt, and R. Henderson, "Hardware implementation algorithm and error analysis of high-speed fluorescence lifetime sensing systems using center-of-mass method." Journal of biomedical optics **15**, 017006 (2010).
12. N. Sorokin, "Implementation of high-speed fixed-point dividers on FPGA," Journal of Computer Science Technology **6**, 8–11 (2006).
13. ISS Fluorescence and Biomedical Instrumentation, *Lifetime Data of Selected Fluorophores Data Tables* (2015).
14. L. Braga, M. Perenzoni, and D. Stoppa, "Effects of DCR, PDE and saturation on the energy resolution of digital SiPMs for PET," in "Nuclear Science Symposium and Medical Imaging Conference (NSS/MIC), 2013 IEEE," (2013), pp. 1–4.